

## Equation of State of Nuclear Matter in the Relativistic Dirac-Brueckner Approach

Bernard ter Haar and Rudi Malfliet

*Kernfysisch Versneller Instituut, University of Groningen, 9747 AA Groningen, The Netherlands*

(Received 13 December 1985)

Within the framework of the relativistic Dirac-Brueckner approach, the equation of state of nuclear matter is studied on the basis of a one-boson-exchange interaction. The saturation properties of the ground state and its compressional energy are calculated. The model is extended to nonzero temperature by use of finite-temperature Green's functions for the dressed nucleons. Isotherms in a  $P$ - $\rho$  diagram are obtained which show the existence of a liquid-vapor phase equilibrium below a critical temperature of  $T_c \approx 12$  MeV.

PACS numbers: 21.65.+f

The equation of state of nuclear matter describes the behavior of a system of nucleons at different temperatures and densities. Besides the mean field calculations of Walecka,<sup>1</sup> the first microscopic calculations were based on a Hartree-Fock approximation with use of an effective nucleon-nucleon ( $NN$ ) interaction, particularly a Skyrme interaction.<sup>2</sup> The major disadvantage, however, of the Skyrme-type interactions is that they are not well established away from the saturation point and even there they give far too high a value for the compression modulus. Microscopic calculations of the full equation of state based on a realistic free  $NN$  interaction have so far only been performed within a variational description.<sup>3</sup> Both types of calculations show a liquid and a gas phase of nuclear matter with a critical temperature of about 17 MeV at half of normal nuclear density.

While the equation of state of nuclear matter for  $T \neq 0$  is relatively unexplored, many microscopic calculations, however, are performed on the ground state of nuclear matter. Besides other methods, its saturation properties have been extensively studied via the Brueckner-Bethe-Goldstone approach. Nonrelativistic calculations of this type, based on realistic  $NN$  interactions, were, however, not very successful in describing the saturation energy and density of nuclear matter, unless three-body forces were explicitly included.<sup>4</sup> Extensions to finite temperatures are rare and up to now rather limited.<sup>5-7</sup> Recently several relativistic Brueckner calculations on saturation properties have been performed.<sup>8-10</sup> New in these calculations is that the nucleon in the nuclear medium is described by an effective Dirac spinor wave function, which yields in fact a different saturation mechanism. In this Letter we shall present a relativistic Dirac-Brueckner (DB)

calculation on the full equation of state of nuclear matter based on a one-boson-exchange (OBE) interaction. It is along the same line as the calculation of Ref. 10, where only the ground-state saturation properties are studied. We will extend our model to finite temperature and show some properties of the equation of state.

The  $NN$  interaction within a nuclear medium is given by the effective  $t$  matrix  $\Gamma$ , which in relativistic field theory is a solution of the medium-dependent Bethe-Salpeter equation

$$\Gamma = K + i \int KGG\Gamma. \quad (1)$$

Here  $K$  is the full two-body kernel and  $G$  is the interacting nucleon propagator that obeys the Dyson equation

$$G(k) = G^0(k) + G^0(k)\Sigma(k)G(k), \quad (2)$$

where  $G^0$  is the noninteracting propagator and  $\Sigma(k)$  the nucleon self-energy. This self-energy is the result of the effective interaction of a nucleon with all the other nucleons of the medium, which in the Brueckner approach can be expressed as

$$\Sigma(k) = -i \int [\text{tr}(G\Gamma) - G\Gamma]. \quad (3)$$

This set of equations is practically unsolvable. Several reductions have to be made to get a scheme that is numerically feasible. In our actual calculation we follow the method given by Horowitz and Serot.<sup>9</sup> The Bethe-Salpeter equation is commonly reduced to a three-dimensional covariant quasipotential equation. We will use the Thompson approximation,<sup>11</sup> which differs only in detail from the more familiar Blankenbecler-Sugar approximation. The equation for  $\Gamma$  can be written as

$$\langle \mathbf{p}'s'_{i2} | \Gamma | \mathbf{p}s_{12} \rangle = \langle \mathbf{p}'s'_{i2} | U | \mathbf{p}s_{12} \rangle + \sum_{s'_{i2}} \int \frac{d^3\mathbf{p}'}{(2\pi)^3} \langle \mathbf{p}'s'_{i2} | U | \mathbf{p}'s'_{i2} \rangle \frac{Q(\mathbf{p}', P, s^*)}{E_{p'}^{*2} (\frac{1}{2}s^{*1/2} - E_{p'}^* + i\epsilon)} \langle \mathbf{p}'s'_{i2} | \Gamma | \mathbf{p}s_{12} \rangle, \quad (4)$$

where  $U$  gives the quasipotential and  $Q$  is the relativistic (angle-averaged) Pauli exclusion operator which depends not only on the relative momentum in the two-particle center-of-momentum frame  $\mathbf{p}'$ , but also on the total momentum  $P$  and total invariant mass  $s^*$  of the two particles in the nuclear-matter rest frame. The spin values of

particles 1 and 2 are given by  $s_{12}$ . The asterisks in this equation display the influence of the nucleon self-energy. This can be shown by writing the full Green's function  $G(k) = \{\mathbf{k} - m - \Sigma(k)\}^{-1}$  as  $G(k) = \{\mathbf{k}^* - m^*\}^{-1}$ , which is based on the general expression of  $\Sigma(k)$ ,

$$\Sigma(k) = \Sigma_S(k) - \gamma_0 \Sigma_0(k) - \boldsymbol{\gamma} \cdot \mathbf{k} \Sigma_V(k). \quad (5)$$

Dirac-Hartree-Fock calculations show that the  $k$  dependence of  $\Sigma$  is very weak and that the vector part  $\Sigma_V$  is much smaller than the other two.<sup>9</sup> Therefore we can write

$$k_\mu^* = k_\mu + \delta_{\mu 0} \Sigma_0, \quad E_k^* = (\mathbf{k}^2 + m^{*2})^{1/2}, \quad (6)$$

where the effective mass  $m^*$  is determined from<sup>9</sup>

$$m^* = m + \Sigma_S(k) - m^* \Sigma_V(k)$$

at  $k = k_F$ , the Fermi momentum. In fact, Eq. (4) is written down with use of this approximation. The quasipotential now contains effective Dirac spinors

$$u(p^*, \sigma) = \frac{E^* + m^{*1/2}}{2m^*} \begin{pmatrix} 1 \\ \frac{\boldsymbol{\sigma} \cdot \mathbf{p}}{E^* + m^*} \end{pmatrix} X_\sigma. \quad (7)$$

Usually Eq. (4) is solved in a partial-wave-helicity frame. Instead we calculate  $\Gamma$  in full momentum-spin space, reducing Eq. (4) to a two-dimensional integral equation by the use of rotational symmetry. In order for us to calculate  $\Sigma(k)$  [Eq. (3)], the effective  $t$  matrix  $\Gamma$  has to be transformed from the  $NN$  c.m. frame to the nuclear-matter rest frame. To achieve this,  $\Gamma$  can be projected on five covariant interaction matrices, the scalar, vector, tensor, axial-vector, and pseudovector interactions. We choose here a pseudovector instead of a pseudoscalar interaction in contrast to Ref. 9, but in accordance with our choice for the one-pion exchange, as has been discussed in Tjon and Wallace and Horowitz.<sup>12</sup> After self-consistent solutions for  $\Gamma$  and  $\Sigma(k)$  are obtained, the energy density of the medium is given by

$$\epsilon = \sum_{k \leq k_F} \langle \bar{u}(k^*) | [\boldsymbol{\gamma} \cdot \mathbf{k} + m + \frac{1}{2} \Sigma(k)] | u(k^*) \rangle. \quad (8)$$

TABLE I. Parameters of the OBE interaction.<sup>a</sup>

Meson	Mass (MeV)	$I, J^P$	$g_\alpha^2/4\pi$	$f_\alpha/g_\alpha$
$\pi$	139	$1, 0^-$	14.16	
$\omega$	784	$0, 1^-$	11.7	0.0
$\rho$	764	$1, 1^-$	0.43	5.1
$\epsilon$	571	$0, 0^+$	7.8	
$\eta$	550	$0, 0^-$	2.0	
$\delta$	962	$1, 0^+$	1.43	

<sup>a</sup>  $\Lambda^2 = 1.3 \text{ GeV}^2$ .

Equation (4) is solved numerically by use of the Padé-approximant method. As input for the quasipotential  $U$  a one-boson-exchange interaction is used. Nucleonic excitations like the  $\Delta(3,3)$  are left out here, although they might cause important effects. In the near future we will present calculations including  $\Delta$  degrees of freedom. As mentioned before we apply pseudovector  $\pi$  exchange besides  $\epsilon$ -,  $\omega$ -,  $\eta$ -,  $\rho$ -, and  $\delta$ -meson exchange. To account for the finite size of the nucleon a monopole vertex form factor  $\Lambda^2/(\Lambda^2 + q^2)$  is included. The parameters given in Table I are chosen such that free  $NN$  phase shifts, differential cross sections, and polarization data up to  $E_{\text{lab}} = 250$  MeV are nicely reproduced, as is the deuteron binding energy. These results will be presented elsewhere. Our code has been checked by recalculating the Blankenbecler-Sugar results of Zuilhof and Tjon<sup>13</sup> for all phase shifts, and the Brueckner calculations of Ref. 9.

In Fig. 1 the binding energy of nuclear matter is displayed as a function of the density. The full curve represents the self-consistent solution of Eqs. (4), (5), and (8), in which all medium effects are taken into account in the intermediate nucleon states as well as in their external lines. To show the influence of the use

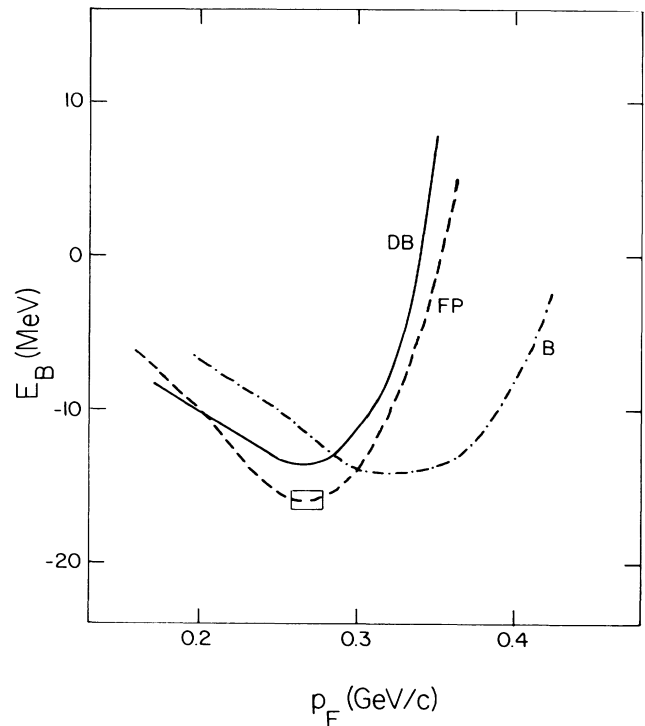


FIG. 1. Energy per nucleon in nuclear matter vs the Fermi momentum  $k_F$ . Comparison of the Dirac-Brueckner result (DB, full line) with the variational calculation of Ref. 4 (FP, dashed line) and a conventional Brueckner calculation (B, dash-dotted line) as described in the text.

of effective Dirac spinors this result is compared with a "pseudoconventional" Brueckner calculation. For this we put in Eq. (4)  $m^* = m$  and modify the two-body Green's function to  $(\frac{1}{2}\sqrt{s} - E_p + \Sigma_S - \Sigma_0)^{-1}$  which is comparable to the "standard choice" in conventional Brueckner theory. In this way a self-consistency condition still remains which is essential for a fair comparison. The main conclusion that can be drawn from Fig. 1 is that the DB model gives a lower saturation density, very near the "empirical" value. In Fig. 1 we also compare our DB results with the variational calculation of Friedman and Pandharipande (FP) and find a remarkable equivalence. One should notice here that these authors phenomenologically include a density-dependent term in the interaction, which they call a three-body force. Within the DB approach the interaction is also density dependent but in an intrinsic way by means of the effective spinors. At higher densities the difference between the DB and FP results grows, as is shown in Fig. 2, where the compressional energy is displayed for densities up to 4 times saturation density. Both curves have a compression modulus of  $K = 250$  MeV at the saturation point. At higher densities the DB curve becomes stiffer. This is partly due to the approximation on Eq. (8) in which only the self-energy at the Fermi surface enters:  $\Sigma(k_F)$ . Taking into account the full  $k$  dependence of  $\Sigma$  in the interior of the Fermi sea leads to the dashed curve of Fig. 2, called DB'.

The Dirac-Brueckner approach can also be applied at finite temperatures. The major modification is the inclusion of finite-temperature Green's functions<sup>14</sup> for the nucleons. The step functions  $\theta(k_F - |\mathbf{k}|)$  are replaced by the full occupation density

$$n_k = \{\exp[(E_k^* - \mu^*)/T] + 1\}^{-1}, \quad (9)$$

where  $\mu^*$  is fixed by the density  $\rho$ . Similarly the two-body Green's function can be reduced to an effective one-body propagator and a temperature-dependent exclusion operator  $Q$ .<sup>15</sup> Because the pole in the effective

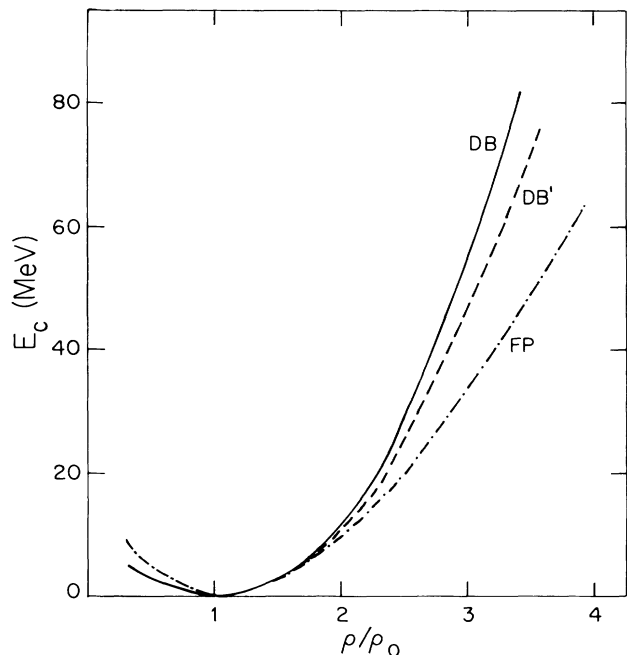


FIG. 2. Compressional energy per nucleon in nuclear matter vs the medium density  $\rho$  for the Dirac-Brueckner calculation (full line) and the variational calculation of Ref. 4 (dash-dotted line). The influence of the momentum dependence of the self-energy  $\Sigma$  is shown by the comparison of the full and the dashed line.

one-body propagator now enters the integration domain of the intermediate states, the  $\Gamma$ -matrix elements and thus  $\Sigma$  become complex. The imaginary part of  $\Sigma$ , as we have checked explicitly, turns out to be small. Therefore we use the quasiparticle approximation and neglect  $\text{Im}\Sigma$  everywhere, whereas  $\text{Re}\Sigma$  is evaluated at the Fermi momentum  $k_F$ , which is determined by the relation  $E_{k_F}^* = \mu^*$ . In the DB approach self-consistent solutions are obtained for the self-energy  $\Sigma(k, T, \rho)$  and the occupation density  $n_k$ . This enables us to calculate the free energy  $F$  in terms of the internal energy  $U$  and the entropy  $S$ :

$$F(\rho, T) = U(\rho, T) - TS(\rho, T), \quad (10)$$

$$U(\rho, T) = \epsilon/\rho - m, \quad (11)$$

$$S(\rho, T) = \frac{-1}{\rho} \int \frac{d^3k}{(2\pi)^3} \{(1 - n_k) \ln(1 - n_k) + n_k \ln(n_k)\}. \quad (12)$$

The free energy  $F(\rho, T)$  completely describes the thermodynamics of the system. It may be differentiated, for example, with respect to the density to yield the pressure  $P(\rho, T)$ :

$$P(\rho, T) = \rho^2 \partial F(\rho, T) / \partial \rho. \quad (13)$$

With the same OBE interaction as given before we calculated isotherms of nuclear matter in a  $P$ - $\rho$  diagram,

displayed in Fig. 3. The results are in good overall agreement with the variational calculations as well as the Skyrme-Hartree-Fock calculations. A liquid-vapor phase equilibrium is observed at low densities and low temperatures. The critical temperature we deduce is  $T_c \approx 12$  MeV and it is positioned at a density  $\rho_c \approx 0.6\rho_0$ . This critical point is remarkably closer to the

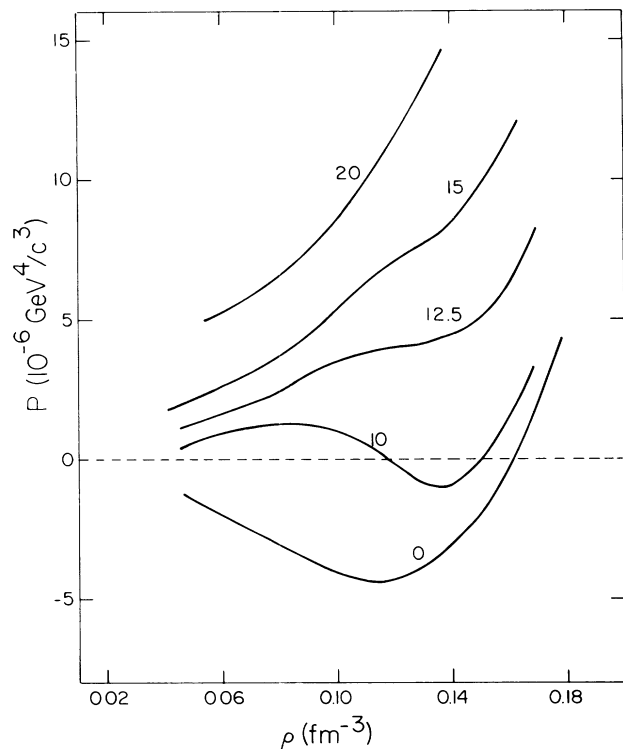


FIG. 3. The nuclear-matter isotherms in a pressure-density ( $P$ - $\rho$ ) diagram for temperatures  $T = 0, 10, 12.5, 15,$  and  $20$  MeV.

ground state than was calculated before. In agreement with Ref. 3 we found only a very small temperature dependence of  $m^*$ .

In conclusion, we have presented a calculation of the equation of state of nuclear matter within the Dirac-Brueckner approach. Starting from a OBE interaction which fits free  $NN$  data, very reasonable saturation and compressibility values are obtained for the nuclear-matter ground state. The compressional energy at higher density indicates rather stiff behavior.

We extended the Brueckner scheme to  $T \neq 0$  using finite-temperature Green's functions for the dressed nucleons and found a liquid-gas phase equilibrium below a critical temperature of  $T_c \approx 12$  MeV.

<sup>1</sup>J. D. Walecka, *Ann. Phys.* **83**, 491 (1974); R. A. Freedman, *Phys. Lett.* **71B**, 369 (1977).

<sup>2</sup>G. Sauer, H. Chandra, and U. Mosel, *Nucl. Phys.* **A264**, 221 (1976); J. M. Lattimer, *Annu. Rev. Nucl. Part. Sci.* **31**, 337 (1981), and references therein.

<sup>3</sup>K. E. Schmidt and V. R. Pandharipande, *Phys. Lett.* **87B**, 11 (1979); B. Friedman and V. R. Pandharipande, *Nucl. Phys.* **A361**, 502 (1981).

<sup>4</sup>B. D. Day, *Rev. Mod. Phys.* **50**, 495 (1978), and *Comments Nucl. Part. Phys.* **11**, 115 (1983).

<sup>5</sup>J. R. Buechler and S. A. Coen, *Astrophys. J.* **212**, 807 (1977).

<sup>6</sup>R. K. Tripathi, *Phys. Rev. C* **25**, 1114 (1982).

<sup>7</sup>A. Lejeune, P. Grange, M. Martzoff, and J. Cugnon, to be published.

<sup>8</sup>M. R. Anastasio, L. S. Celenza, and C. M. Shakin, *Phys. Rev. C* **23**, 2273 (1981); M. R. Anastasio, L. S. Celenza, W. S. Pong, and C. M. Shakin, *Phys. Rep.* **100**, 327 (1983).

<sup>9</sup>C. J. Horowitz and B. D. Serot, *Phys. Lett.* **137B**, 287 (1984); B. D. Serot and J. D. Walecka, in *Advances in Nuclear Physics Vol. 16*, edited by E. Vogt (Plenum, New York, 1986).

<sup>10</sup>R. Brockmann and R. Machleidt, *Phys. Lett.* **149B**, 283 (1984); R. Machleidt and R. Brockmann, *Phys. Lett.* **160B**, 364 (1985).

<sup>11</sup>R. H. Thompson, *Phys. Rev. D* **1**, 110 (1970); R. Woloshyn and A. Jackson, *Nucl. Phys.* **A185**, 131 (1972).

<sup>12</sup>J. A. Tjon and S. J. Wallace, *Phys. Rev. Lett.* **54**, 1357 (1985); C. J. Horowitz, *Phys. Rev. C* **31**, 1340 (1985).

<sup>13</sup>M. J. Zuilhof and J. A. Tjon, *Phys. Rev. C* **24**, 735 (1981).

<sup>14</sup>A. L. Fetter and J. D. Walecka, *Quantum Theory of Many-Particle Systems* (McGraw-Hill, New York, 1971).

<sup>15</sup>E. S. Fradkin, *Nucl. Phys.* **12**, 465 (1959).